Journal of Engineering and Sustainable Development
www.jeasd.org
Vol. 20, No.05, September 2016
ISSN 2520-0917

SELECTING OF AN EFFECTIVE ADSORBENT FOR TREATING PHOSPHATE CONTAMINATION

*Dr. Ahmed Hassoon Ali[1], Younis Swadi Tlaiaa [2], Lahieb Faisal M. Ali[3], Ali Qasim Rdhaiwi[4]

1) Asst. Prof., Environmental Engineering Department, Al-Mustansiriayah University, Baghdad, Iraq.
2) Asst. Lect., Environmental Engineering Department, Al-Mustansiryah University, Baghdad, Iraq
3) Asst. Lect., Environmental Engineering Department, Al-Mustansiryah University, Baghdad, Iraq
4) Eng., Environmental Engineering Department, Al-Mustansiryah University, Baghdad, Iraq

Abstract: Experimental researches on adsorptive capacity of: Granular Activated Carbon GAC, Phosphate Rock PR, Saw Dust SD and Rice Husk RH for phosphate removal from simulated wastewater were conducted. Results showed that removal efficiency of four adsorbents were in the consequence as: RR (82.6%) > SD (43.72%) > GAC (41.28%) > RH (34.4%). To understand the action of phosphate uptake, factors influencing the adsorption process using best adsorbent (PR) including pH, mixing speed, contact time, weight of the adsorbent, initial phosphate concentration and temperature were investigated. It was found that the equilibrium data fitted very well to the Langmuir model with high determination coefficient (R^2). The maximum uptake capacity (q_{max}) was 24.716 mg/g. Adsorption data were modeled using the pseudo-first, pseudo-second-order, Intraparticle diffusion and Elovich models. It was found that, the pseudo- second-order kinetic equation could best describe the adsorption kinetics. Thermodynamic parameters showed that the adsorption of investigated phosphate onto PR was exothermic, spontaneous in nature and the process is physiosorption. It was found that sodium hydroxide (0.1 M NaOH) was efficient desorbent solution in recovery of phosphate pollutant among different desorbents: HCl, H_2SO_4, NaOH, Na_2CO_3, EDTA and deionized distilled water (DDW) from PR. The breakthrough curves for the adsorption column test was obtained in a continuous adsorption fixed-bed experiment, The measured breakthrough times for RH, GAC, SD and PR were found to be 10, 30, 40 and 60 min, respectively.

Keywords: *Adsorption, Phosphate, GAC, PR, , RH.*

اختيار ماده ممتزه فعالة لإزالة تلوث الفوسفات

الخلاصة: تم في هذه الدراسة بحث القابلية الامتزازية لكل من : الكاربون المنشط الحبيبي (GAC)، الصخور الفوسفاتية (PR)، نشارة الخشب (SD) وقشور الرز (RH) لإزالة الفوسفات من المياه الملوثة المصنعة. لقد بينت النتائج ان كفاءه الازالة لكل من المواد الممتزة الاربعة هي على النحو التالي: الصخور الفوسفاتية (82.6%) > نشارة الخشب (43.72%) > الكاربون المنشط الحبيبي > (41.28%) > قشور الرز (34.4%). ولفهم آليه أزاله الفوسفات فان العوامل المؤثرة على عمليه الامتزاز باستخدام أفضل مادة ممتزة (الصخور الفوسفاتية) متضمنه كل من : الرقم الهيدروجيني ، سرعة المزج، وقت التلامس، وزن المادة الممتزة، التركيز الابتدائي ودرجة الحرارة سوف يتم اختبارها. لقد تم اكتشاف ان النتائج العملية تنطبق بصورة جيدة جداً مع النموذج الرياضي لانكمير وبمعامل ارتباط عالي وكانت أكبر سعة امتزاز (q_{max}) 24.716 ملغم/غم .نتائج الامتزاز تم تطبيقها على موديلات الحركة من الدرجة الاولى، الثانية، الانتشار الداخلي ومودیل أيلوفج حيث بينت النتائج ان موديل الحركة من الدرجة الثانية يمثل نتائج الامتزاز بصورة جيدة. محددات الحرارة التي تم ايجادها لعملية امتزاز الفوسفات على الصخور الفوسفاتية بينت ان العملية تلقائية وفيزيائية بطبيعتها. لقد تم ايجاد ان هيدروكسيد الصوديوم (0.1M) هو الأكفأ في استعاده الفوسفات من الصخور الفوسفاتية من بين عده محاليل اعاد امتزاز هي HCl, H_2SO_4, NaOH,

*Corresponding Author ahmedhassoon_2021@yhoo.com

DDW ، Na_2CO_3, EDTA. منحنيات الانكسار لعمود الامتزاز تم الحصول عليها من تجارب الامتزاز ذات النمط المستمر. اوقات منحنيات الانكسار تم ايجادها لكل من RH, GAC, SD and PR لتكون ١٠، ٣٠، ٤٠ و ٦٠ دقيقة على التوالي.

1. Introduction

Wastewater containing phosphate should be treated before discharge to eliminate the possible. To protect aquatic quality, waste water containing phosphate must be treated to meet the discharge limit for phosphate [1, 2 and 3]. As this discharge limit is becoming more and more stringent, even further treatment of the effluent is required. When the input of phosphorus to waters is higher than it can be assimilated by a population of living organisms the problem of excess phosphorus content occurs. Regulatory control on phosphorus disposal is evident all over the world in recent years. Strict regulatory requirements decreased the permissible level of phosphorus concentration in wastewater at the point of disposal (i.e. 1 mg/L). This has made it very important to find appropriate technological solution for treatment of wastewater prior to disposal.

Conventional phosphorus removal methods from wastewater include chemical precipitation [4], biological processes [5, 6], reverse osmosis [7] and sorption processes [8, 9]. Among these techniques, adsorption is a promising method to treat waste water, especially at lower phosphate concentrations, which pose a challenge to the use of the traditional flocculation methods [10]. In recent decades, booming studies have been focused on the selection of ideal adsorption materials [11, 12, 13 and 14]. In order to eliminate the possible dangers to receiving water sources, it is necessary to treat before discharge. Adsorption of phosphate from aqueous solution has been studied in the past few decades by several authors using different adsorbents, like activated alumina [15], half-burnt dolomite [16], activated carbon [17], coconut shell carbon [18], clays [19], bentonite [20], ferrihydrite [21], goethite [22], and hematite [23].

The objective of this study was to select an effective adsorbent from conventional and nonconventional adsorbents for the removal of phosphate from simulated wastewater. The influences of different experimental parameters such as solution pH, dosage, contact time, temperature, initial concentration on phosphate removal as well as phosphate desorption were also investigated. Moreover, phosphate adsorption mechanism was elucidated in this paper.

2. Materials and methods

2.1. Adsorbents preparation

Four different types of adsorbents are used: commercial granular activated carbon (GAC), rise husk (RH), phosphate rocks (PR) and sawdust (SD). Commercial granulated activated carbon (GAC) was supplied by (Unicarbo, Italians) and was bought from the Iraqi markets. The activated carbon was washed before being used with distilled water to remove fine powder and then dried in an oven at 110 ^{o}C for 24 hours, after which the GAC is kept in a desiccators for use. The rice husk (RH)was collected from Al-Shamiyyah rice mill located in Al-Diwaniya where large amounts of residual

rice husk were produced in production of rice. The rice husk was filtered and washed with excess distilled water and dried in an oven at 60°C for 24 hours. The phosphate rock (PR) comes from the Akashat phosphate mines located in the western region of Iraq, about 110 km west of the capital Baghdad. The choice of this material is based on its low cost, considering its abundance in the Iraqi ores. Iraq is one of the major courtries in phosphate production. The amount of phosphate production in Iraq was about 1,199,343 tons/year [24]. The PR was crushed and washed with excess distilled water and dried in an oven at 110°C for 24 hours.

The Sawdust (SD) was collected from several furniture factories in Baghdad where large amount are produced as residuals from production of different furniture. This was washed with double distilled water to remove water-soluble impurities and surface-adhered particles. Then the adsorbent was oven-dried at 60^{o}C for 24 hours to remove the moisture and other volatile impurities. The GAC, RH, PR and SD samples was sieved into mesh 0.6, 1 mm using Germany sieves. For non-spherical particles, the particle diameter is defined as the equivalent diameter of a spherical particle with the same volume. As an approximation, the particle diameter may be calculated from the geometric mean of the two consecutive sieve openings without introducing serious errors. The geometric mean diameter is given by, $d_{gm} = (d_1 d_2)^{1/2}$, where d_1 is the diameter of the lower sieve on which the particles are retained and d_2 is the diameter of the upper sieve through which the particles pass [25].

The physical and chemical properties of adsorbents are measured at the laboratories of the Ministry of Industry and Minerals (Ibn Sina State Company), Ministry of Oil (Petroleum Development and Research Center), Al-Mustansiriaya University (College of Engineering, Environmental Department) and according to the data from the supplier and listed in Table 1.

Table 1. Adsorbents specifications

Specifications	*Adsorbents*			
	GAC	RH	PR	SD
Source	Uncarbo company Italy form local markets	Local Iraqi mills	Akashat phosphate mines	Collected from a local furniture factory
Bulk density (real density) (kg/m^3)	641 (1544)	233.52 (1390)	674.56 (2500)	462.05 (1509)
Surface area (m^2/g)	351.965	136.69	607.53	10.1712
Porosity %	53.44	83.2	36	69.38
Pore volume (cm^3/g)	0.422	0.054	0.437	Nil
*CEC (meq/100g)	-	43.118	-	116.8

*Cation Exchange Capacity

The specific surface area and total pore volume were measured using the multi-point-N2-Brunauer, Emmett and Teller (BET) method (Surface area analyzer, BET method, Quantachrome.com, USA). The functional groups of PR was detected by FT-IR analysis. The proportion of adsorbent/KBr is 1/100. The background is obtained from

the scan of pure KBr. FT-IR spectrophotometer, IRPRESTIGE-21, SHIMADZU, Japan was used for analysis. Phases present in the samples (chemical analysis) were analyzed using an X-ray diffractometer (PAN analytical X-ray, Philips Analytical, Germany) and present in Table 2.

Table 2 Chemical analysis of GAC, RH, PR and SD samples

GAC		*R.H*		*PR*		*S.D*	
Constituent	Wt.%	constituent	Wt.%	constituent	Wt.%	constituent	Wt.%
C	88.77	SiO_2	96.36	P_2O_5	25.47	SiO_2	86.1
O	10.51	MgO	0.4	CaO	52.29	$CaSiO_3$	2.9
Si	0.28	Al_2O_3	0.42	MgO	0.7	MgO	2.6
S	0.05	K_2O	2.30	Fe_2O_3	16.5	Al_2O_3	4.4
K	0.18	CaO	0.42	SiO_2	3.5	SO3	2.1
Ca	0.21	Fe_2O_3	0.1	L.O.I	1.54	L.O.I*	1.9
*Loss Of Ignition							

2.2. Preparation of phosphate solution

All chemicals are analytical grade and used without further purification. Reaction vessels (glass) were cleaned with 1 % HNO_3 and rinsed several times with deionized water before use. Phosphate stock solution was prepared by dissolving the anhydrous potassium dihydrogen orthophosphate (KH_2PO_4) in deionized water. Phosphate working solutions were freshly prepared by diluting phosphate stock solution with appropriate amounts of deionized water.

2.3. Batch experiments

In order to select the best adsorbent from GAC, RH, PR and SD in removing of phosphate from simulated wastewater. Four glass bottles of 300 mL volume contains 100 mL solution of initial concentration C_o 50 mg/L, the pH was fixed at 4 using 0.1 M NaOH or HNO_3 solution. The dose of each adsorbent was 1 gm. The glass bottles were then placed on a shaker (HV-2 ORBTAL, Germany) and agitated continuously for 4 hr at 200 rpm and 30 ^oC. The samples filtered by 42 Whatman filter paper [26]. The final equilibrium concentrations were measured by means of spectrophotometer device.

The removal efficiency (adsorption efficiency) is calculated by the difference in the initial and final concentration of each phosphate by the following relationship:

$$R(\%)=\frac{(C_o - C_e)}{C_o}\times 100 \quad (1)$$

Where C_o and C_e are the initial and final concentration respectively (mg/L). The experiments are repeated triple and the average concentration was taken.

2.4 Fixed bed experiments

The fixed-bed breakthrough curve was measured by a continuous adsorption experiment. An acrylic column of (50 mm) inner diameter and (0.5 m) height was

packed with 100 g adsorbent as shown in Fig. 1. There was a distributor on the top of the column in order to allow a homogeneous flow distribution. Porous organic plastic supports were used to hold the carbons in the column. Phosphate initial concentration solution of 50 mg/L was pumped through the carbon bed at the rate of 2.78×10^{-6} m^3/s using a peristaltic pump (BT-100, China). Effluent samples were taken at various times for phosphate concentration analysis.

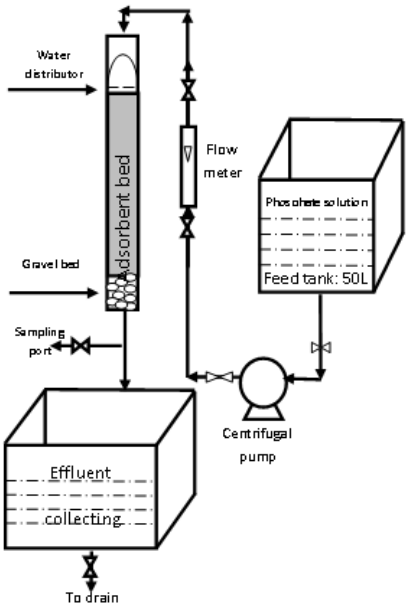

Figure 1. Schematic diagram of the experimental set up fora continues process.

3. Results and discussion

3.1 Selection the best adsorbent

The removal efficiency of phosphate ions using GAC, RH, PR and SD are shown in Fig. 2. As shown from this Figure that, the removal efficiency of phosphate onto tested adsorbents follows the sequence as: PR > SD > GAC > RH

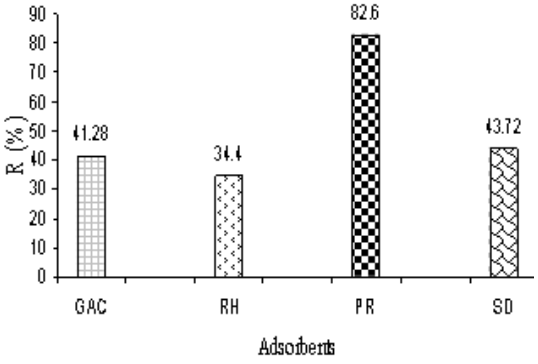

Figure 2. Removal efficiency of phosphate onto different adsorbents, C_o 50 mg/L, pH 4, adsorbent dose 1 g per 100mL and temperature 30 ^{o}C.

PR has more surface area than other adsorbents as determined in Table 1. Consequently, more adsorption sites are available for phosphate ions adsorption. On the other hand, cation exchange capacity (CEC) for SD that represents the total amount of phosphate ions that can be replaced by positive ions (K^+, Na^+, Ca^{2+}, and Mg^{2+}) on SD. CEC for SD used in this study was 116.8 meq/100 g. Thus, adsorption capacity for SD exceeds that for RH. Consequently, PR will be used as adsorbent in next batch experiments.

3.2. *FTIR analyses of PR*

In order to find out which functions are responsible for the phosphate adsorption, FT-IR analysis of PR was carried out. Figure 3 shows the spectra of raw and treated phosphate samples. The sharp bands near 435.91, 921.97, and 1145.72 define the Si–OH stretches [27]. The peak at 875.68 cm^{-1} is associated with the PO_4^{-3} group. The bands between 1000 and 1095.57 cm^{-1} are Si-O and those at 1427.32, 1454.33, and 1635.64 are C=O, and at 1998.25–2357.01 are P-H. The sharp peaks at 3641.60 and 3448.72 are O-H stretching. All peaks defined above are related to the mineralogical composition of the sorbent (PO_4, SiO_2, and CO_3) [28]. Peak displacement decrease defines the change in the structure with phosphate, implying that the related functional groups are responsible for the adsorption process.

Table 3 shows the main functional groups before and after phosphate rocks were loaded with phosphate ions. The results show that, the bands of carboxylic (C=O) groups shifted to lower frequency and thus considered the most important functional groups in the adsorption of phosphate onto PR. The bands of functional groups shifted to lower frequency with a total amount of 78.89.

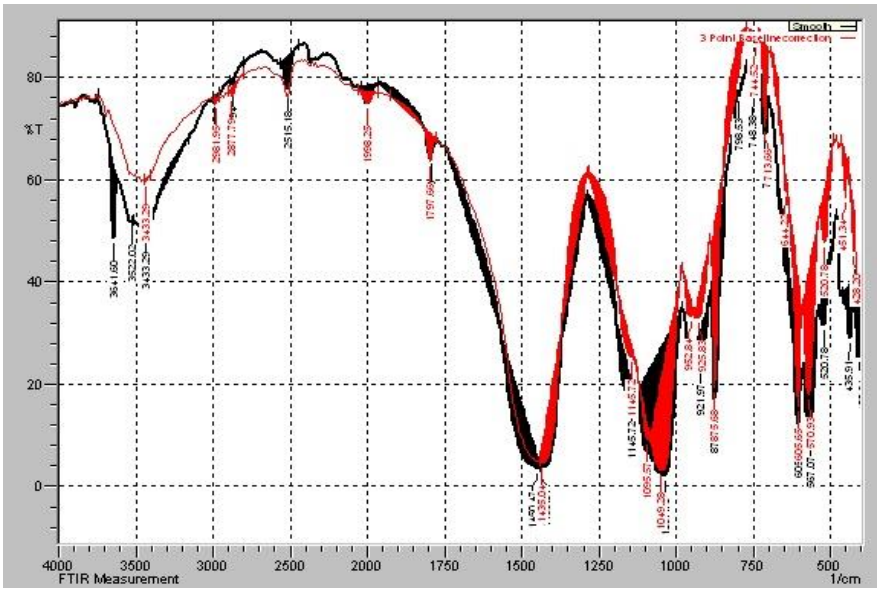

Figure 3. FT-IR spectra of PR (-) before, (-) after phosphate adsorption

Table 3. Functional groups before and after PR was loaded with phosphate ions

Assignment groups	Unloaded, cm^{-1}	Loaded with phosphate, cm^{-1}	Δ
Hydroxyl (¯OH)	3641.60	3634.35	7.25
	3448.72	3443.21	5.51
Summation			12.76
Phosphine (p-H)	2357.01	2353.85	3.16
	2017.54	2012.78	4.76
	1998.25	1996.21	2.04
Summation			9.96
Carboxylic (C=O)	1635.64	1619.34	16.3
	1454.33	1443.54	10.79
	1427.32	1417.9	9.42
Summation			36.51
Silanol (Si–OH)	1157.29	1153.97	3.32
	929.69	923.75	5.94
	493.78	488.86	4.92
Summation			14.18
Siloxane (Si-O)	1095.57	106.42	3.15
Phosphate (PO_4^{-3})	876.78	873.45	3.33
Total summation			78.89

3.3. *Determination of optimum conditions for PR performance*

3.3.1 Effect of pH

The influence of pH on the removal efficiency for phosphate is shown in Figure ٤. As cleared from this figure, the phosphate uptake was evidently dependent on pH with the greatest adsorption occurring under acidic conditions and decreased with increase in solution pH [29]. For example, the phosphate PO_4^{3-} removal rate decreased from 88.65 % around pH 3 to about 34.62 % at pH 9. Similar pH effect on phosphate ions adsorption by iron or iron-based oxides has been reported by a number of authors [29]. Such phenomenon could be explained as follows: negative charged $H_2PO_4^-$ and HPO_4^{2-} are dominant phosphate species in the solution under the tested pH range (3–9). Lower pH is favoring the protonation of PR surface and increased protonation is thought to increase the positively charged sites, enlarge the attraction force existing between the PR surface and phosphate ions and therefore increase the amount of adsorption in the lower pH region. As solution pH increase, the negatively charged sorptive sites dominate gradually and more negatively charged phosphate species are also becoming dominant, which enhances the repulsion effect between the PR and the phosphate ions. Therefore, the amount of phosphate uptake is consequently dropped.

The point of zero charge pH (pH_{PZC}) study also confirms the increase of phosphate elimination with a pH of round 3. The pH at point zero charge (pH_{PZC}) of the prepared

PR was determined by the solid addition method. The pH_{PZC} of a material in a solution is the pH value at which the net surface charge of this material is equal to zero. Below this pH (pH=4 in the present study as shown in Fig. ٥) the adsorbent functional group is protonated and the adsorbent surface is positively charged; however, adsorption of negatively charged ions is favorable. In the simplest interpretation, hydrogen ions become winners in this competition. Above this pH, these groups deprotonate and the adsorbent surface becomes negatively charged, so in this region of pH phosphate ions cannot be attracted effectively onto the PR surface [30].

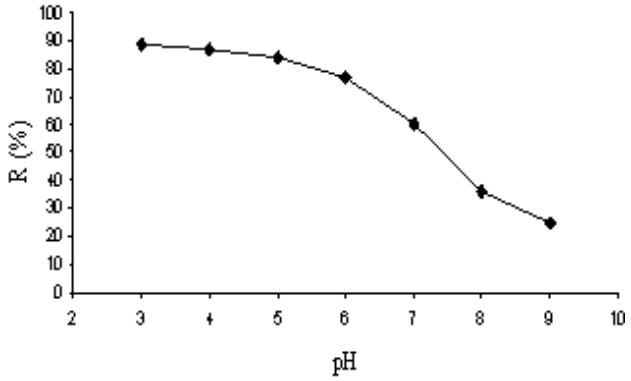

Figure 4. Effect of pH on the adsorption of phosphate onto PR at C_o= 50 mg/L, mixing speed=200 rpm, contact time = 4 h, PR dose=0.5 g/100mL and temperature= 30 ^{o}C

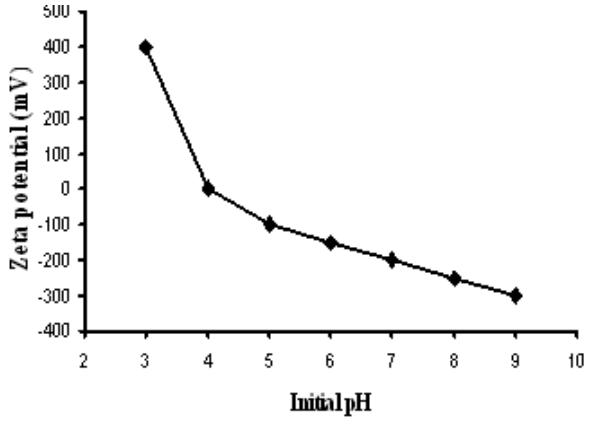

Figure 5. pH point of zero charge (pH_{PZC})

3.3.2 Effect of mixing speed

The effect of the mixing speed on the removal efficiency of phosphate using PR is shown in Fig.5. The efficiency value increase from: 45.32 to 90.34 % as the agitation speed increased from 50 to 250 rpm. The mixing speed increases the percentage removal efficiency until it reaches a fixed value and further increase is then of no benefit (i.e., above 250 rpm). The increase in percentage efficiency is due to the increase in turbulence and this decrease the external mass transfer resistance thickness around the adsorbent particles with increase in mixing speed by reducing the boundary layer thickness to a minimum value [31]. These results indicate that a mixing speed of 250 rpm is sufficient to obtain maximum removal efficiency.

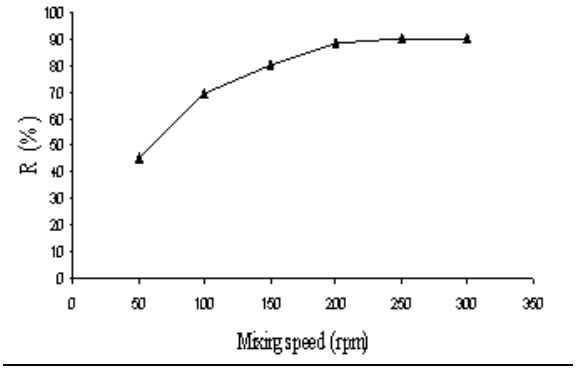

Figure 6. Effect of mixing speed on the adsorption of phosphate at C_o= 50 mg/L, pH= 3, contact time = 4 h, adsorbent dose=1g/100mL and temperature= 30 ^{o}C.

3.3.3 Effect of PR dose

The effect of varying the adsorbent dose (mass) on the adsorption of various metal ions is shown in Fig. 7. It is clearly seen that the removal efficiency increases as the PR mass increases. As the PR mass increases, the number of binding sites for the phosphate ions also increases. After some point (2.5 g), adsorption capacity was steady due to a screen effect between adsorbent, this produced a block of the adsorbent active sites by an increase of adsorbent (PR) in the system [32]. Similar observations were also made by other investigators [33, 34]. Removal efficiency increases from: 79.45 to 96.78% as the PR dose increased from 0.5 to 2.5 g. Thus, in next experiments, the optimum dosage was fixed at 2.5 g.

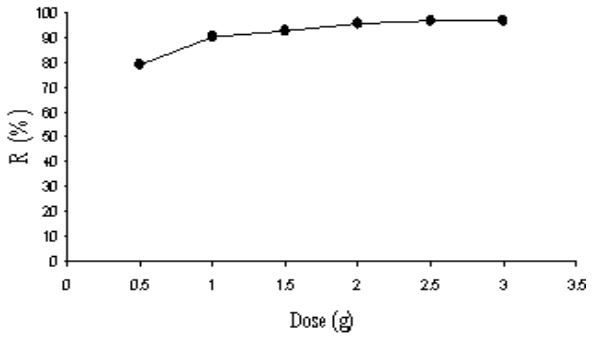

Figure 7. Effect of adsorbent on the adsorption of phosphate onto PR at C_o= 50 mg/L, pH= 3, contact time = 4 h, mixing speed=250 rpm and temperature = 30 ^{o}C.

3.3.4 Effect of contact time

Contact time plays an important role in the efficient removal of phosphate using PR. Therefore, the adsorption of phosphate at constant temperature, initial concentration, best mixing speed, best adsorbent dose and best pH was studied as a function of contact time to determine the equilibrium time. The influence of contact time on the adsorption capacity is shown in Fig.8. Removal efficiency increases from 15.35 to 97.88% as the contact time increases from 30 to 270 min. The results revealed that rate of adsorption is higher at the beginning and this is due to availability of a large number of active sites on the adsorbent. As these sites are exhausted, the uptake rate is controlled by the rate at

which the adsorbate is transported from the exterior to the interior sites of the adsorbent particles [35]. Maximum removals were attained with in the first 240 min of stirring time. There must not be seemed to be much benefit after 270 min. Therefore the equilibrium time was set to be 270 min in further experiments.

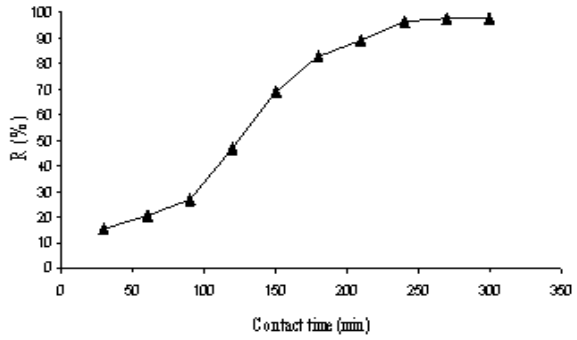

Figure 8. Effect of contact time on the adsorption of phosphate onto PR at C_o= 50 mg/L, pH= 3, dose = 2.5 g/100 mL, mixing speed=250 rpm and temperature= 30 ^oC.

3.3.5 Effect of initial concentration

The experiments were performed at distinct initial concentrations ranging from 25 to 100 mg/L. As shown in Fig. 9, the efficiency values decreases from: 98.65 to 80.75 % as the initial concentration increased from 25 to 100 mg/L. This is due to the lack of binding sites in the PR sample for the adsorption of metal ions at higher concentrations. The effect of initial metal concentration could be explained as follow: at low metal ion/adsorbent ratio, metal ion adsorption involves higher energy binding sites. As the metal ion/adsorbent ratio increase (i.e., at higher initial concentration), the higher energy binding sites are saturated and adsorption begins on lower energy binding sites, resulting in decrease in the adsorption efficiency [36].

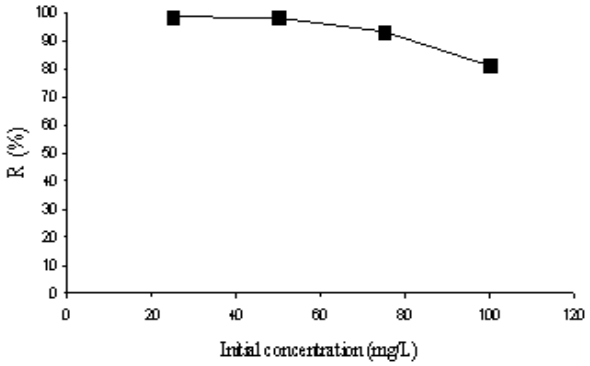

Figure 9. Effect of initial concentration on the adsorption phosphate onto PR at pH= 3, mixing speed=250 rpm, dose= 2.5g/100 mL, contact time = 4.5h and temperature= 30 ^oC

3.3.6 Effect of temperature

Fig. 10 shows the adsorption efficiency of phosphate onto PR at six different temperatures of 10, 20, 30, 40, 50 and 60 ^oC. It can be seen that as the temperature increases, the adsorption capacity decreased. For instance, for an initial concentration 50 mg/L the adsorption efficiency of the adsorbent decreases from 99.43 to 88.98 % as the

temperature increase from 10 to 60 ^{o}C. This means that, as the temperature increased the rate of desorption was more significant than the rate of adsorption, which implies that adsorption is an exothermic reaction, a well-known scientific fact [37].

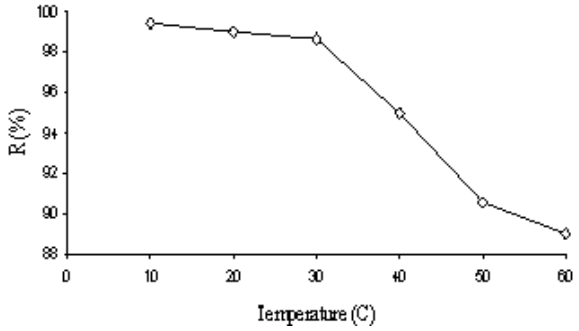

Figure 10. Effect of temperature on the adsorption of phosphate onto PR at C_o= 50 mg/L, pH= 3, mixing speed=250 rpm, t adsorbent dose= 2.5g/100mL, contact time = 4.5h.

3.4 *Adsorption isotherm*

The adsorption isotherm for phosphate onto PR is shown in Figure 11. The obtained data have been correlated with five models. The parameters for each model which obtained from non-linear statistical fit of the equation to the experimental data (Statistica-v6) are summarized in Table 4.

From Fig. 11 and Table 4, the following conclusions can be drawn: Langmuir model gave the best fit for the experimental data for phosphate adsorption with correlation coefficients of 0.994. This indicates that the adsorption process occurs as a mono layer. The maximum adsorbed amount (q_m) is 24.716 mg/g. A comparison of the maximum adsorption capacity (q_m) of the PR sample with that of some other adsorbents reported in the literature is given in Table 5. The adsorption capacity of the PR samples was relatively high when compared with other adsorbents.

Table 4. Parameters of adsorption isotherm for phosphate ions onto PR

Model	Equation	Parameters	Values	Reference
Freundlich	$q_e = KC_e^{1/n}$	K, (mg/g)(L/mg)$^{(1/n)}$	1.231	[38]
		n	1.249	
		R^2	0.895	
Langmuir	$q_e = \frac{q_m b C_e}{1+bC_e}$	q_m, (mg/g)	24.716	[39]
		b, (L/mg)	0.046	
		R^2	0.994	
Reddlich–Peterson	$q_e = \frac{A_R C_e}{1+B_R C_e^{m_R}}$	A_R, mg/g L/mg	0.1336	[40]
		B_R, (L/mg)^{mR}	-0.897	
		m_R	-0.034	
		R^2	0.915	
Sips	$q_e = \frac{bq_m C_e^{1/n}}{1+bC_e^{1/n}}$	q_m, (mg/g)	140.820	[41]
		b, (L/mg)	0.008	
		n	1.208	
		R^2	0.925	
Khan	$q_e = \frac{Q_{max} b_k C_e}{(1+b_k C_e)^{a_k}}$	Q_{max}, (mg/g)	0.044	[35]
		b_K, (L/mg)	65.231	
		a_K	0.200	
		R^2	0.901	

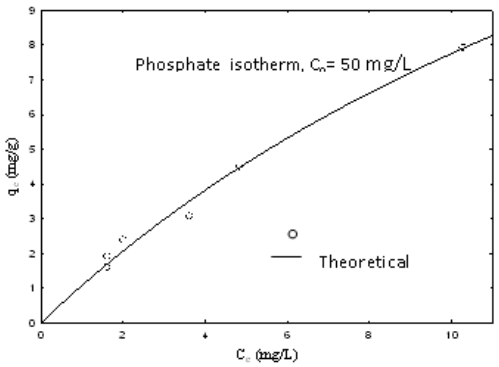

Figure 11. Adsorption isotherm for phosphate onto PC

Table (5) Adsorption capacities (q_m, mg/g) for phosphate ions of various adsorbents

Adsorbent	q_m, mg/g	References
Mesoporous ZrO2	29.7	[42]
Red mud	0.23	[43]
Hydrous niobium oxide	4	[44]
Magnetic Fe–Zr binary oxide	13.6	[45]
Hydrous niobium oxide	13	[46]
Akaganéite	49	[47]
PR	24.716	Present study

3.5 Kinetic model

The kinetics of phosphate adsorption onto PR was analyzed using pseudo-first-order, pseudo-second-order, intra-particle diffusion, and Elovich kinetics models from time. Table 6 and Fig.12 demonstrate the results of these models and the following conclusions can be achieved:

- Pseudo-second order was the most fitted model to experimental data. The adsorption uptake equal to 7.758 mg/g, this is closed to the experimental uptake of 7.025 for phosphate ions, respectively with R^2 of 0.986.
- The value of constant (C) in the intra-particle diffusion model is not equal to zero, suggesting that adsorption proceeds from boundary layers mass transfer across the interfaces to the intra-particle diffusion within the pores of adsorbent. This indicates the mechanisms of metal ions adsorption is complex and both the surface adsorption as well as intra-particle diffusion contribute to the rate determining step [48].

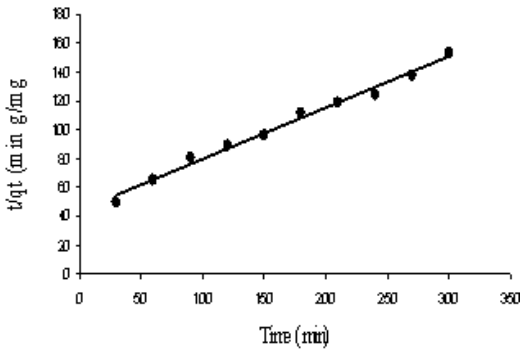

Figure 12. Pseudo-second order model for adsorption of phosphate ions onto PR.

Table 6. Kinetic model parameters for phosphate adsorption onto PR

Model	Equation	Parameters	Value
Pseudo-first-order	$\log(q_{eq}-q_t)=\log q_{eq}-(\frac{k_L t}{2.303})$	q_{eq}(mg/g)	33.014
		K_L(1/min)	0.030
		R^2	0.826
Pseudo-second-order	$\frac{t}{q_t}=\frac{1}{k_s q^2_{eq}}+\frac{t}{q_{eq}}$	q_{eq} (mg/g)	7.758
		K_s(g/mg.min)	3.44×10^{-3}
		R^2	0.986
Intraparticle Diffusion	$q_t=k_{id}t^{1/2}+C$	C	1.864
		K_{id}(mg/g.min$^{0.5}$)	0.358
		R^2	0.934
Elovich	$q_t=\frac{1}{b}\ln a\bar{b}+\frac{1}{b}\ln t$	a(mg/g.min)	0.88
		b^- (g/mg)	0.784
		R^2	0.912

3.6 *Adsorption Thermodynamics*

Based on fundamental thermodynamic concepts, it is assumed that in an isolated system, energy cannot be gained or lost and the entropy change is the only driving force. The apparent equilibrium constant for the process has been shown to be [39]:

$$\Delta G^o = -RT\ln Kc \tag{14}$$

$$K_c = \frac{C_o - C_{eq}}{C_{eq}} \tag{15}$$

Also, enthalpy changes (ΔH^o) and entropy changes (ΔS^o) can be estimated by the following equation:

$$\Delta G^o = \Delta H^o - \Delta S^o T \tag{16}$$

where ΔG° is the standard Gibbs free energy change in kJ/mol; ΔH° is the change in enthalpy (heat of adsorption, kJ/mole), ΔS° is the change in entropy in kJ/mol, R is the universal gas constant (=8.314 J/mol.K) and T is the temperature in K. Table 7 and Fig. 13 show the thermodynamic constants of adsorption for phosphate onto PR. The value of enthalpy ΔH° was −34.765 kJ/mol, suggested the physiosorption and exothermic nature of adsorption. This is also supported by the decrease in the values of uptake capacity of adsorbent with the rise in temperature. The value of entropy ΔS was -0.0872 J/mol K, reflect the affinity of phosphate ions to be adsorbed onto PR. The negative values of G° confirm the feasibility of the process and the spontaneous nature of adsorption [40].

Table 7. Thermodynamic parameters for the adsorption of phosphate onto PR.

Temperature, K	$-\Delta G^o$, kJ/mol	$-\Delta H^o$, kJ/mol	$-\Delta S^o$, J/mol.K	R^2
383	9.828	34.768	0.0872	0.975
393	9.485			
303	8.234			
313	7.875			
323	6.447			
333	5.622			

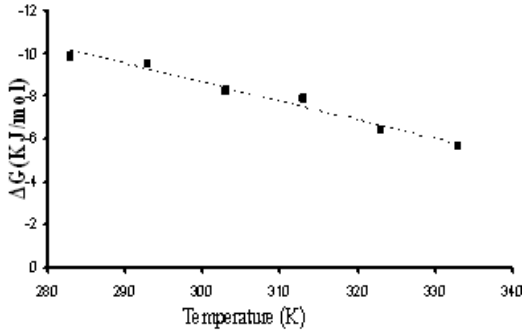

Figure13. Free energy change for phosphate adsorption.

3.7 *Desorption and regeneration*

Desorption experiments were performed in order to demonstrate the ability of spent selected adsorbent for regeneration and reuse. Desorption of phosphate ions from loaded PR was carried out by solvent elution, using 0.1M of HCl, H_2SO_4, NaOH, Na_2CO_3, Ethylenediaminetetraacetic acid (EDTA) and deionized distilled water (DDW) as an eluents. The desorption of phosphate ions were carried out from each 1 g of loaded adsorbent which had previously adsorbed phosphate in experiments of effect of adsorbent dosage and dried, with initial concentration of 50 mg/L. It was carried out by 50 mL of elute for 4.5 h shaking in a batch system at 250 rpm. Volume of elutant solution was selected to achieve complete immersing and good mixing of solid particles.

Thereafter, the desorbed ions was analyzed and the eluting efficiencies of the desorbents $E_{d.}$ are calculated according to Eq. (17). The most efficient elutant was then used in consecutive adsorption–desorption–regeneration cycle.

The desorption efficiencies using the different desorbing elutants from PR are calculated from Eq. below:

$$E_{d.}(\%) = \frac{m_{d.}}{m_{ad.}} = \frac{C_{d.} \times V_e}{C_{ads.} \times V_L} \quad (17)$$

Where C_d, C_{ads} are the adsorbed and desorbed concentrations (mg/L); V_e, V_L are the elutant and phosphate solutions volumes (mL). The results are listed in Table 8 and shown in Fig. 14. It is clear from the previous Figure and Table that, the elution tendency as a percentage recovery of metal ions followed the sequence as:
NaOH > Na_2CO_3 > EDTA > H_2SO_4 > HCl > DDW

NaOH and Na_2CO_3 found to be the most efficient elutants in desorbing of phosphate ions. This observed trend may be due to affinity between negative ions present in phosphate and NaOH. Sodium hydroxide is considered one of the chelating agents which interact with phosphate through molecular attraction through covalent bond, which is stronger than that responsible to bind phoshate to functional groups onto PR surface. A similar conclusion was given by Qadeer and Rehan, 1998 [49].

Table 8. Desorption efficiency of the different elutants.

Elutant (0.1 M)	Desorption of Phosphate from PR; V_e=50 mL, V_L= 100 mL $C_{ads.}$= 48.638 mg/L	
	$C_{d.}$ (mg/L)	$E_{d.}$(%)
HCl	7.724	7.940
H_2SO_4	10.068	10.349
NaOH	94.698	97.350
Na_2CO_3	93.608	96.229
EDTA	86.534	88.957
DDW	7.192	7.393

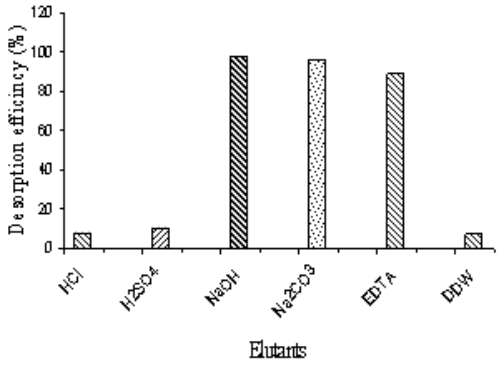

Figure 14. Phosphate recovery from PR

4. Column Experiments (Continuous Process)

The fixed-bed breakthrough curve was obtained by a continuous adsorption experiment. It can be seen from Fig. 15 that all phosphate were initially retained in the fixed- bed because of full adsorption (no phosphate in the effluent). With greater phosphate solution flow through the bed, the phosphate concentration in the effluent increases steadily until it reaches the same value as its inlet concentration (C_o), the so-called breakthrough point, when the fixed-bed is saturated. The measured breakthrough times for RH, GAC, SD and PR are 10, 30, 40 and 60 min, respectively. These results proved that those obtained in batch system where (PR) is adsorbed phosphate ions more strongly than other types of adsorbents. The bed-depth service-time model (BDST) is used to estimate the required bed depth for a given service-time. The BDST model can be expressed as below [50]:

$$t_b = \frac{N_o}{C_i u} Z - \frac{1}{C_i K} \ln\left(\frac{C_i}{C_b} - 1\right) \quad (18)$$

where C_b is the solute concentration in the effluent of the column at breakthrough (at 10% breakthrough point , i.e. t_b at C_b=5 mg/L), C_i is the solute concentration in the effluent to the column (50 mg/L), N_o is the adsorption capacity, Z is the bed height (0.05 m), u is the superficial velocity (3.37×10^{-7} m/sec) and K is the rate constant which represents the solute transfer from the liquid phase to the solid phase (mg/L.min). The parameters N_o and K for BDST model were obtained from nonlinear statistical fit of the equation to the experimental data (Statistica, v6) which are summarized in Table 9. The R^2 value mostly close to unity indicating the suitability of the BDST model to represent the adsorption of phosphate in a fixed-bed of PR, SD, GAC and RH. The adsorption capacity N_o as shown in Table 9 for PR is higher than that for other adsorbents. This result proved the results obtained in batch system for maximum adsorption capacity (q_m). This models has been used successfully by other researchers to estimate the required depth for a specific adsorption time [51].

Table 9. Parameters predicted from the BDST model for adsorption of phosphate on tested adsorbents.

Type of carbon	N_o, mg/L	K, L/mg.min	R^2
PR	153.5	0.00023	0.982
SD	156	0.00044	0.990
GAC	164	0.00083	0.979
RH	190	0.00101	0.979

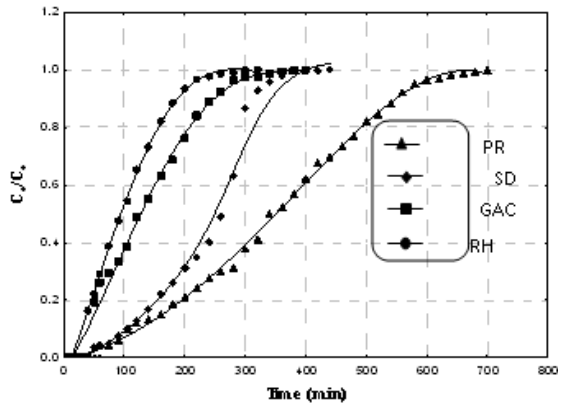

Figure 15. Fixed- bed breakthrough curve for PR, SD, GAC and RH

5. Conclusions

The study showed numbers of conclusions during batch and continuous experiments for adsorption of phosphate ions solutions.

1. Removal efficiency by PR greater than that of SD, GAC and RH for the phosphate ions removal.
2. Optimum pH, mixing speed, adsorbent dosage and contact time were 3, 250 rpm, 2.5 g and 270 min respectively.
3. Removal efficiency decreased with increasing initial concentration and temperature this is due to the lack of binding sites in the PR sample for the

adsorption of phosphate ions at higher concentrations and increased the rate of desorption at high temperature.

4. Langmuir isotherm gives the best fit model for representing the experimental data for this system.
5. Pseudo-second-order was best model to predict the kinetic process for the phosphate adsorption.
6. Adsorption of phosphate ions was exothermic and physical in nature.
7. Alkaline solution such as NaOH and Na_2CO_3 seem to be successful for phosphate desorption with high desorption efficiency.
8. Experimental data, after adsorption column study, fits well to linear form of BDST model. The equation can be modified to make suitable for a different flow rate and effluent phosphate concentration.

6. References

1. Puckett, L., (1995)."*Identifying the major sources of nutrient water pollution. Environmental Science Technology*", Vol. 29, pp. 408–414.
2. Zhao, D., Sengupta, A., (1998). "*Ultimate removal of phosphate from wastewater using a new class of polymeric ion exchangers*". Water Research, Vol. 32, pp. 1613–1625.
3. Ugurlu, A., Salman, B., (1998). "*Phosphorus removal by fly ash*". Environment International, Vol. 24, pp. 911–918.
4. Donnert, D., Salecker, M., (1999). "*Elimination of phosphorus from waste water by crystallization*". Environmental Technology, Vol. 20, pp. 735–742.
5. De La Noue, J., de Pauw, N., (1988). "*The potential of microalgal biotechnology: a review of production and uses of microalgae*". Biotechnology Advances, Vol. 6, pp. 725–770.
6. De-Bashan, L., Bashan, Y., (2004). "*Recent advances in removing phosphorus from wastewater and its future use as fertilizer*". Water Research, Vol. 38, pp. 4222–4246.
7. Van Voorthuizen, E., Zwijnenburg, A., Wessling, M., (2005)."*Nutrient removal by NF and RO membranes in a decentralized sanitation system*". Water Research, Vol. 39, pp. 3657–3667.
8. Morse, G. K., Brett, S. W., Guy, J. A., Lester, J. N., (1998). "*Review: phosphorus removal and recovery technologies*". Science of the Total Environment, Vol. 212, pp. 69–81.
9. Kang, S., Choo, K., Lim, K., (2003). "*Use of iron oxide particles as adsorbents to enhance phosphorus removal from secondary wastewater effluent*". Separation Science and Technology, Vol. 38, pp. 3853–3874.
10. Seida, Y., Nakano, Y., (2002). "*Removal of phosphate by layered double hydroxides containing iron".* Water Research, Vol. 36, pp. 1306–1312.
11. Agyei, N., Strydom, C., Potgieter, J., (2000). "*An investigation of phosphate ion adsorption from aqueous solution by fly ash and slag*". Cement and Concrete Research, Vol. 30, pp. 823–826.

12. Khelifi, O., Kozuki, Y., Murakami, H., Kurata, K., Nishioka, M., (2002). "*Nutrients adsorption from seawater by new porous carrier made from zeolitized fly ash and slag*". Marine Pollution Bulletin, Vol. 45, pp. 311–315.
13. Tanada, S., Kabayama,M., Kawasaki, N., Sakiyama, T., Nakamura, T., Araki, M., Tamura, T., (2003). "*Removal of phosphate by aluminum oxide hydroxide*". Journal of Colloid and Interface Science, Vol. 257, pp. 135–140.
14. Zeng, L., Li, X., Liu, J., (2004). "*Adsorptive removal of phosphate from aqueous solutions using iron oxide tailings*". Water Research, Vol. 38, pp. 1318–1326.
15. Brattebo, H., Odegaard, K. (1986). "*The influence of different substrates on enhanced chemical phosphorus removal in a sequencing batch reactor*". J. Water Res., Vol. 20, pp. 977-981.
16. Roques, H., Jeddy, N., Libuglf, A., (1991). "*Phosphorus removal from wastewater by half-burned dolomite*". Water Res., Vol. 25, pp. 959-965.
17. Koh, K.J., Chung, G. J., (1998). "*Phosphorus removal and recovery technologies*". Hwahok Kanghok, Vol. 23, pp. 303-308.
18. Palanivelu, K., Elangovan, N., (1994). "*Removal of Phosphorus from solutions using coconut shell carbon".* Indian J. Environ. Prot., Vol. 14, pp. 688-695.
19. Fox, I., (1993). "*Using different caly types in phosphate removal processes*", J. Chem. Technol. Biotechnol., Vol. 57, pp. 97-101.
20. Gonzalez-Pradas, E., Sanchez, M.V. and Allego Campo, G.A. (1992). "*Removal of Phosphorus from aqueous solutions using bentonite as an adsorbent*". J. Chem. Technol. Biochenol. Vol. 54, pp. 291-297.
21. Hawka, D., Carpenter, P. D., Hunter, K. A., (1989). "*Synthetic routes for preparation of good adsorbents for phosphorus removal*". Environ. Sci. Technol., Vol. 23, pp. 187-191.
22. Parfitt, R. L.,(1989). "*Studying the adsorption properties of goethite towards phosphorus and nitrogen removal*". J. Soil Sci., Vol. 40, pp. 359.
23. Colombo, C., Barren, V., Torrent, J., (1994). "*Using hematite in phosphate removal from its waste streams*". Geochim. Cosmochim. Acta, Vol. 58, pp. 1261-1266.
24. Setatnia, A., Madami, A., Bakhti, M.Z., Keryous, L., Mansouri, Y., Yous, R., (2004). "*Biosorption of Ni^{2+} from aqueous solution by a NaOH treated bacterial dead Streptomices rimosus biomass*". Miner. Eng., Vol. 17, pp. 903–911.
25. Alexander, P. M., Zayas, I., (1989). "*Particle size and shape effects on adsorption rate parameters*". Environ. Eng., Vol.115, pp. 41–55.
26. APHA, (1995). "*Standard methods for the examination of water & wastewater*", 19th Edition, American Public Health Association, Washington, DC.
27. Ma, QY., Traina, SJ., Logan, TJ., Ryan, JA., (1995). "*Lead immobilisation from aqueous solutions and contaminated soils using phosphate rocks*". Environ. Sci. Technol. Vol. 29, pp. 1118–1126.
28. Soejoko, DS., Tjia, MO., (2002). "*Infrared spectroscopy and X-ray diffraction study on the morphological variations of carbonate and phosphate compounds in giant prawn (Macrobrachium rosenbergii) skeletons during its moulting period*". J. Mater. Sci. Vol. 38, pp. 2087–2093.

29. Zhang, G. S., Liu, H. J., Liu, R. P., Qu, J. H.,(2009). "*Removalof phosphate from water by a Fe–Mn binary oxide adsorbent*". Journal of Colloid and Interface Science, Vol. 335, pp.168– 174.
30. Zubeyde, B., Ercan, C., Mehmet, D., (2009). "*Equilibrium and thermodynamic studies on biosorption of Pb(II) onto Candida albicans biomass*". J Hazard Mater, Vol. 161, pp. 62–67.
31. Yasemin, B., Tez, Z.,(2007). "*Adsorption studies on ground shells of hazelnut and almond".* J. Hazazrdous Materials, Vol. 149, No.1, pp. 35-41.
32. Ali, A.H., (2013). "*Comparative study on removal of cadmium(II) from simulated wastewater by adsorption onto GAC, DB, and PR*". Desalination and Water Treatment J., Vol.1, pp.1-12.
33. Hammaini, A., Ballester, F. A., Blazquez, M.L., Munoz, J.A., (2006). "*Biosorption of heavy metals by activated sludge and their desorption characteristics*". J. Environ. Manage., Vol. 84, No. 4, pp. 419-426.
34. Kumar, S.D., Subbaiah, V. M., Reddy, A. S., Krishnaiah, A.,(2009). "*Biosorption of phenolic compounds from aqueous solutions onto chitosan-abrus precatorius blended beads*". J Chem Technol Biotechnol., Vol. 84, pp. 972-981.
35. Vijayaraghavan, K., Yun, Y-S.,(2008). "*Bacterial biosorbents and biosorption*". Biotechnol Adv, Vol. 26, pp. 266–291.
36. Al-Qodah, Z.,(2006). "*Biosorption of heavy metal ions from aqueous solutions by activated sludge*". Desalination, Vol.196, pp. 164-176.
37. Sag, Y. and T. Kutsal, (2000). "*Determination of the biosorption heats of heavy metal ions on Zoogloea and Rhizopus arrhizus*". Biochem. Eng. J., Vol.6, pp. 145-151.
38. Gupta, VK., Rastogi A., (2008). "*Equilibrium and kinetic modeling of cadmium (II) biosorption by nonliving algal biomass Oedogonium sp. from aqueous phase*". J Hazard Mater, Vol. 153, pp. 759–766.
39. Sulaymon, HA., Abidb AB., Al-Najar AJ., 2009. Removal of lead copper chromium and cobalt ions onto granular activated carbon in batch and fixed-bed adsorbers. Chem Eng J., 155(3), 647–653.
40. Quintelas, C., Fernandes, B., Castro J, Figueiredo H, Tavares, T.,(2008). "*Biosorption of Cr(VI) by three different bacterial species supported on granular activated carbon—a comparative study*". J Hazard Mater, Vol. 153, pp. 799–809.
41. Özer, A., (2003). "*Comparative study of the biosorption of Pb(II), Ni(II) and Cr(VI) ions onto S. cerevisiae: determination of biosorption heats*". J Hazard Mater, Vol. 100, pp. 219–229.
42. Liu, B. and R. T. Baker (2008). "*Factors affecting the preparation of ordered mesoporous ZrO2 using the replica method*". J. Mater. Chem., Vol.18, pp. 5200–5207.
43. Huang W, Wang S, Zhu Z, Li L, Yao X, Rudolph V, et al., (2008). "*Phosphate removal from wastewater using red mud*". Journal of Hazardous Materials, Vol. 158, No. 1, pp. 35--42.

44. Ye, H. P., Chen, F. Z., Sheng, Y. Q., Sheng, G. Y., & Fu, J. M. (2006). "*Adsorption of phosphate from aqueous solution onto modified palygorskites*". Separation and Purification Technology, Vol. 50, pp. 283–290.
45. Long, F., Gong, J.-L., Zeng, G.-M., Chen, L., Wang, X.-Y., Deng, J.-H., Niu, Q.-Y., Zhang, H.-Y., & Zhang, X.-R. (2011). "*Removal of phosphate from aqueous solution by magnetic Fe–Zr binary oxide*". Chemical Engineering Journal, Vol. 171, pp. 448–455.
46. Rodrigues, L. A., & Silva, M. L. C. P. D. (2009). "*An investigation of phosphate adsorption from aqueous solution onto hydrous niobium oxide prepared by co-precipitation method*". Colloids and Surfaces A: Physicochemical and Engineering Aspects, Vol. 334, pp. 191–196.
47. Deliyanni, E. A., Peleka, D. N., & Lazaridis, N. K. (2007). "*Comparative study of phosphates removal from aqueous solutions by nanocrystalline akaganéite and hybrid surfactant– akaganéite*". Separation and Purification Technology, Vol. 52, pp. 478–486.
48. Ali, A.H., (2011). "*Performance of Adsorption/Biosorption for Removal of Organic and Inorganic Pollutants*", Thesis, University of Baghdad, college of engineering.
49. Qadeer, R., Rehan, A., (2002). "*A Study of the Adsorption of Phenol by Activated Carbon from Aqueous Solutions*". Turk J Chem., Vol. 26, pp. 357–361.
50. Muhamad, H., Doan and A. Lohi, (2012). "*Batch and fixed bed column biosorption of Cd^{+2} and Cu^{2+} ",* chemical engineering journal, Vol. 158, pp.369-377.
51. Muhamad, H., Doan, H., Lohi, A., (2012). "*Batch and fixed bed column biosorption of Cd^{+2} and Cu^{2+} ",* chemical engineering journal, Vol. 158, pp. 369-377.